

Title	Passivation effect of ultra-thin SiN _x films formed by catalytic chemical vapor deposition for crystalline silicon surface
Author(s)	Song, Hao; Ohdaira, Keisuke
Citation	Japanese Journal of Applied Physics, 57(8S3): 08RB03-1-08RB03-4
Issue Date	2018-06-11
Type	Journal Article
Text version	author
URL	http://hdl.handle.net/10119/16132
Rights	This is the author's version of the work. It is posted here by permission of The Japan Society of Applied Physics. Copyright (C) 2018 The Japan Society of Applied Physics. Hao Song and Keisuke Ohdaira, Japanese Journal of Applied Physics, 57(8S3), 2018, 08RB03. http://dx.doi.org/10.7567/JJAP.57.08RB03
Description	

**Passivation effect of ultra-thin SiN_x films
formed by catalytic chemical vapor deposition
for crystalline silicon surface**

Hao Song and Keisuke Ohdaira*

Japan Advanced Institute of Science and Technology (JAIST),

Nomi, Ishikawa 923-1292, Japan

*E-mail: ohdaira@jaist.ac.jp

We propose a way of replacing silicon dioxide (SiO₂) films in tunnel oxide passivated contact (TOPCon) solar cells by ultra-thin Si nitride (SiN_x) films. We deposit SiN_x films on n-type crystalline Si (c-Si) wafers by catalytic chemical vapor deposition (Cat-CVD), by which we avoid a plasma damage to the surface of c-Si. Thin (<5 nm) SiN_x films can be deposited with good controllability by tuning the deposition conditions. To improve the passivation quality of SiN_x films, hydrogen treatment was performed onto the SiN_x-coated c-Si surfaces. Their effective minority carrier lifetime (τ_{eff}) can be improved up to >1 ms by the hydrogen treatment for the samples containing SiN_x with a proper refractive indices and >10-nm-thick n-type amorphous Si (n-a-Si). The ultra-thin SiN_x films have sufficiently high passivation ability and have the required level for the passivation layers of rear-side contact in the TOPCon-like c-Si solar cells.

1. Introduction

Photovoltaic (PV) power generation has been widely popularizing as a major renewable energy resource.^{1,2)} Crystalline silicon (c-Si) wafer-based solar cells claim a significant share of the PV market at present and in the near future, and are thus the most important PV technology.^{3,4)} Nowadays, the structure of the c-Si solar cells has been shifting to that with partial rear contact (PRC) for the sake of reducing the area of a direct metal-semiconductor junction, which shows a significant recombination of carriers. However, for the passivated emitter with rear locally diffused (PERL) cells,⁵⁾ unpassivated contacting area limits open-circuit voltage (V_{oc}) and conversion efficiency due to its high recombination velocity over 10^5 cm/s, even if the ratio of the contacting area is less than 1%.⁶⁾

Recently, solar cells with a full-area carrier-selective contact passivated by tunneling Si dioxide (SiO_2) have been proposed, which are referred to as tunnel oxide passivated contact (TOPCon) cells.⁷⁻¹²⁾ The TOPCon cell contains a tunneling SiO_2 with a thickness of ~ 1.4 nm and a ~ 20 -nm-thick n^+ -Si layer formed on the SiO_2 on the rear side of the cell. The tunneling SiO_2 is thin enough to let carriers tunneling through it. The termination of dangling bonds by the ultra-thin SiO_2 and field-effect passivation induced by the n^+ -Si layer lead to high V_{oc} and conversion efficiency.^{7,10)} Wet-chemical treatment is frequently used for the formation of the ultra-thin SiO_2 in the TOPCon structure,¹⁰⁻¹²⁾ through which SiO_2 layers are grown on both sides of a Si wafer. The additional process for the removal of the SiO_2 grown on the front side will thus be needed.

To solve this problem, we newly propose to replace the tunneling SiO_2 by silicon nitride (SiN_x) formed by chemical vapor deposition (CVD), by which one-side film formation can be easily realized. Furthermore, SiN_x has a narrower bandgap of ~ 5 eV^{13,14)} than that of SiO_2 of ~ 9 eV,¹⁵⁾ which may lead to more efficient carrier tunneling. This means that a thicker tunneling layer can be utilized for CVD SiN_x , which results in better passivation. As the CVD method for the deposition of the thin SiN_x films, we particularly use catalytic CVD (Cat-CVD).^{16,17)} Cat-CVD can realize low-damage deposition of passivation films due to its plasma-damage-less nature, and we have thus far demonstrated high-quality passivation films formed by Cat-CVD.¹⁸⁻²⁴⁾ In this study, we attempt to form ultra-thin SiN_x films aiming at the utilization of the SiN_x as the substitute of tunneling SiO_2 in the TOPCon structure.

2. Experimental methods

We used 20×20 mm²-sized, 290-μm-thick, mirror-polished n-type c-Si(100) wafers with a resistivity of 1-5 Ω·cm as substrates. The wafers first received ultrasonic cleaning in acetone, ethanol and water for 5 min, respectively. Then the wafers were dipped in 5% hydrofluoric acid (HF) to remove native oxide layers. SiN_x films were deposited by Cat-CVD on the cleaned Si wafers under the conditions summarized in Table I. A distance between a wafer holder and a tungsten catalyzer was set to 12 cm in the Cat-CVD chamber. For the experiment of the formation of thin SiN_x films, deposition duration was systematically changed.

For the passivation of c-Si surfaces, SiN_x films were deposited for 30 s under the conditions shown in Table II on the both sides of Si wafers, in which H₂ flow rate is systematically changed and the refractive index and thickness of SiN_x films were varied as a result. We then deposited ~8-nm-thick n-type amorphous Si (n-a-Si) films by Cat-CVD²⁵⁻²⁶⁾ on the SiN_x films. The deposition condition of n-a-Si films is also summarized in Table II. We also fabricated similar passivation structures with n-a-Si films with various thicknesses.

To improve the passivation quality of the thin SiN_x films, atomic hydrogen treatment was performed in the Cat-CVD chamber on the SiN_x films prior to the deposition of n-type a-Si films. The atomic hydrogen treatment was performed at a H₂ flow rate of 20 sccm, at a pressure of 0.2 Pa, and at substrate and catalyzer temperatures of 200 and 1800 °C, respectively.

We measured the thickness and refractive index of SiN_x films by analyzing the data of spectroscopic ellipsometry using the Cauchy model. The passivation quality of SiN_x films was characterized by measuring effective minority carrier lifetime (τ_{eff}) by microwave photoconductivity decay (μ -PCD; KOBELCO LTA-1510 EP) using a microwave with a frequency of 10 GHz and a pulse laser with a wavelength of 904 nm and a photon density of $5 \times 10^{13} \text{ cm}^{-2}$.

3. Results and discussion

3.1 Passivation quality of SiN_x films with different thickness

Figure 1 shows the thickness of SiN_x films as a function of the duration of SiN_x deposition under the condition shown in Table I. The thickness of SiN_x films increases linearly with

deposition duration, and SiN_x films with thicknesses <10 nm can be obtained if we choose deposition durations of <1 min. Figure 2 shows the τ_{eff} of the samples as a function of SiN_x thickness. We can see high τ_{eff} of ≥ 1 ms obtained in the samples with >15-nm-thick SiN_x films. The effective tunneling of majority carriers is, however, not expected in such thick SiN_x films, and comparable τ_{eff} should be realized using much thinner SiN_x films for actual solar cells. The c-Si samples passivated with SiN_x films with a thickness of less than 10 nm, on the contrary, show drastically lower τ_{eff} . There may be two possible reasons for the significant difference in τ_{eff} between the thick and thin SiN_x samples. The first one is the difference of the quality of the SiN_x film at the film/c-Si interface. There might be a ~1-2 nm thick SiON film near the interface, which has a fixed charge density on the order of $\sim 10^{11}$ cm⁻².²⁷⁾ This is lower than the value of $\sim 10^{12}$ cm⁻² for SiN_x,²⁸⁾ and field-effect passivation may be less effective. The second possible reason is that thicker SiN_x films may be able to keep H atoms more effectively during their deposition, which can enhance the termination of dangling bonds on the c-Si surface.

3.2 Hydrogen treatment towards thin SiN_x films

To improve the passivation quality of thin SiN_x films, atomic hydrogen treatment was performed. Figure 3 shows the τ_{eff} of the c-Si samples with <5-nm-thick SiN_x films deposited at a H₂ flow rate of 40 sccm as a function of atomic hydrogen treatment duration. τ_{eff} can be improved up to >300 μs by the atomic hydrogen treatment for ~3 min. We believe that hydrogen atoms supplied during the treatment may pass through the thin SiN_x films and terminate Si dangling bonds on c-Si surfaces. The thicknesses of SiN_x films measured by spectroscopic ellipsometry were 4.45, 4.65, and 4.68 nm for atomic hydrogen treatment durations of 0, 3, and 5 min, respectively. We confirmed that there is no reduction in the thickness of SiN_x films during the hydrogen treatment, showing that the SiN_x films are resistive against atomic hydrogen etching.

3.3 Hydrogen treatment towards thin SiN_x films with various H₂ flow rates

The atomic hydrogen treatment shows an effective improvement in τ_{eff} for the SiN_x films deposited at H₂ 40 sccm and a refractive index of 2.3. The effectiveness of atomic hydrogen treatment is, however, not clear for other SiN_x films with different refractive indices. We thus

performed atomic hydrogen treatment towards SiN_x films deposited at different H₂ flow rates as summarized in Table II.

3.3.1 Variation of the refractive index of SiN_x films depending on H₂ flow rate

Si/N ratio in SiN_x films, to some extent, affects their refractive index.^{29,30)} We varied H₂ flow rate during the deposition of SiN_x films to change their refractive index. Figure 4 shows the thickness and refractive index of SiN_x films as a function of H₂ flow rate during SiN_x deposition. With increasing H₂ flow rate from 0 to 100 sccm, the thickness changes slightly from ~6 to ~4 nm, while refractive index decrease in a wide range from ~2.9 to ~2.0 at a wavelength of 640 nm. The decrease in SiN_x thickness by increasing H₂ flow rate may be due to decrease in the partial pressures of SiH₄ and NH₃. The reason for the decrease in refractive index is the enhancement of the decomposition of NH₃ molecules through vapor-phase reaction with hydrogen atoms—NH₃ + H → NH₂ + H₂.³¹⁾

3.3.2 τ_{eff} variation of c-Si with thin SiN_x films after atomic hydrogen treatment

Based on the variation of the refractive index of SiN_x films shown in Fig. 4, we prepared the samples with different SiN_x films deposited at H₂ flow rates from 0 to 80 sccm for τ_{eff} measurement. We obtained SiN_x films with refractive indices of 2.1–2.9. Atomic hydrogen treatment was then performed in the Cat-CVD chamber prior to the deposition of n-type a-Si films.

Figure 5 shows the τ_{eff} of the c-Si samples passivated with ~5-nm-thick SiN_x films with different refractive indices as a function of atomic hydrogen treatment duration. The c-Si samples passivated with highly Si-rich SiN_x films, with a refractive index of ~2.9, do not gain any τ_{eff} improvement by atomic hydrogen treatment. On the contrary, the τ_{eff} of the other samples passivated with SiN_x films with lower refractive indices can be significantly improved, and the τ_{eff} tends to saturate with increase in atomic hydrogen treatment duration. The τ_{eff} of the c-Si samples passivated with SiN_x films with refractive indices of 2.1 and 2.2 is particularly improved up to >400 μs (~800 μs as the maximum values) by atomic hydrogen treatment. The τ_{eff} improvement is saturated at a treatment duration of ~4 min. The samples with SiN_x with a refractive index of 2.3 show lower maximum τ_{eff} and shorter hydrogen treatment duration for the saturation of τ_{eff} (~3 min). These results indicate that the effect of

atomic hydrogen treatment on τ_{eff} improvement strongly depends on the refractive index of SiN_x films. The reason for the different degree of the effect of the atomic hydrogen treatment might be due to the difference of hydrogen desorption depending on the composition of SiN_x . SiN_x films with more Si content, in general, releases hydrogen more easily,³²⁾ and hydrogen atoms supplied by the hydrogen treatment may be released more frequently. This might also explain the difference of optimum hydrogen treat duration for τ_{eff} improvement. We have also confirmed no reduction in the thickness of SiN_x films with refractive indices of 2.1 and 2.2 by the hydrogen treatment, meaning that these SiN_x films are resistive against hydrogen etching.

3.4 Influence of the thickness of n-a-Si layers on τ_{eff}

The passivation quality of the n-a-Si/ SiN_x stacks may depend also on the properties of n-a-Si films since the existence of the n-type layer induces downward band bending which leads to a decrease in the density of minority carriers near the SiN_x /c-Si interfaces. We thus also investigated the influence of the thickness of n-a-Si films on the quality of the passivation structures. We just change the duration of n-a-Si deposition in Table II. Based on the result shown in Fig. 5, we used SiN_x films with a refractive index of 2.2 receiving atomic Hydrogen treatments for 240 s.

Figure 6 shows the τ_{eff} of the c-Si samples passivated with ~ 5 -nm-thick SiN_x films as a function of n-a-Si thickness. The c-Si samples show τ_{eff} improvement by increasing the thickness of n-a-Si, and τ_{eff} reaches as high as >1 ms in a number of the samples when we use n-a-Si films with thicknesses of ~ 10 nm. The τ_{eff} of the c-Si samples tends to be saturated with further increase in the thickness of n-a-Si films. The increase in τ_{eff} by using thicker n-a-Si films can be understood as more effective downward band bending. Note that we have observed much lower τ_{eff} (<150 μs) in the structures without SiN_x layers.

In this study, we have clarified the importance of the composition of SiN_x films and the thickness of n-a-Si films to realize sufficiently high passivation ability by using the ultra-thin Cat-CVD SiN_x films for the passivation of c-Si surfaces. The highest τ_{eff} obtained in this study is comparable to that for the TOPCon structures.³³⁾ The ultra-thin SiN_x films with a refractive index of 2.1–2.2 and high passivation ability will be applied to the rear-side passivation layers in the TOPCon-like solar cells.

4. Conclusions

We have demonstrated the effectiveness of the passivation of c-Si surfaces with ultra-thin Cat-CVD SiN_x films with a thickness of <5 nm. Drastic reduction in τ_{eff} occurs by reducing the thickness of SiN_x films. However, the passivation quality of the ultra-thin SiN_x films can be significantly improved by atomic hydrogen treatment after SiN_x deposition. The τ_{eff} of the c-Si samples with SiN_x with refractive indices of 2.1 and 2.2 shows particularly large improvement in τ_{eff} up to ~800 μs by the atomic hydrogen treatment. We also confirmed that there is no hydrogen etching of the SiN_x films during the hydrogen treatment. The τ_{eff} of the c-Si samples reach as high as >1 ms by optimizing the thickness of n-a-Si films. The ultra-thin Cat-CVD SiN_x films are thus applicable to the rear contact passivation for TOPCon-like solar cells.

References

- 1) Renewable Electricity: Insights for the Coming Decade
[<https://www.nrel.gov/docs/fy15osti/63604.pdf>]
- 2) S. S. Martin and A. Chebak, *Int. J. Hydrog. Energy* **41**, 21036 (2016).
- 3) 2014 Renewable Energy Data Book [<https://www.nrel.gov/docs/fy16osti/64720.pdf>]
- 4) E. Płaczek-Popko, *Opto-Electron. Rev.* **25**, 55 (2017).
- 5) J. Zhao, A. Wang, P. Altermatt, and M. A. Green, *Appl. Phys. Lett.* **66**, 3636 (1995).
- 6) L. Wang, A. Lochtefeld, J. Han, A. P. Gerger, M. Carroll, J. Ji, A. Lennon, H. Li, R. Opila, and A. Barnett, *IEEE J. Photovoltaics* **4**, 1397 (2014).
- 7) H. Steinkemper, F. Feldmann, M. Bivour, and M. Hermle, *IEEE J. Photovoltaics* **5**, 1348 (2015).
- 8) S. W. Glunz, F. Feldmann, A. Richter, M. Bivour, C. Reichel, H. Steinkemper, J. Benick, and M. Hermle, *Proc. 31st European Photovoltaic Solar Energy Conf.*, 2015, p. 259.
- 9) S. Richter, K. Kaufmann, V. Naumann, M. Werner, A. Graff, S. Großer, A. Moldovan, M. Zimmer, J. Rentsch, J. Bagdahn, and C. Hagendorf, *Sol. Energy Mater. Sol. Cells* **142**, 128 (2015).
- 10) F. Feldmann, M. Simon, M. Bivour, C. Reichel, M. Hermle, and S. W. Glunz, *Sol. Energy Mater. Sol. Cells* **120**, 270 (2014).
- 11) Y. Tao, V. Upadhyaya, K. Jones, and A. Rohatgi, *AIMS Mater. Sci.* **3**, 180 (2016).
- 12) A. Moldovan, F. Feldmann, M. Zimmer, J. Rentsch, J. Benick, and M. Hermle, *Sol. Energy Mater. Sol. Cells* **142**, 123 (2015).
- 13) I. Kobayashi, T. Ogawa, and S. Hotta, *Jpn. J. Appl. Phys.* **31**, 336 (1992).
- 14) S. Miyazaki, M. Narasaki, A. Suyama, M. Yamaoka, and H. Murakami, *Appl. Surf. Sci.* **216**, 252 (2003).
- 15) W. C. Lee and C. M. Hu, *IEEE Trans. Electron Devices* **48**, 1366 (2001).
- 16) H. Matsumura, *Jpn. J. Appl. Phys.* **25**, L949 (1986).
- 17) H. Matsumura and H. Tachibana, *Appl. Phys. Lett.* **47**, 833 (1985).
- 18) K. Koyama, K. Ohdaira, and H. Matsumura, *Thin Solid Films* **519**, 4473 (2011).
- 19) K. Koyama, K. Ohdaira, and H. Matsumura, *Appl. Phys. Lett.*, **97**, 082108(2010)
- 20) T. C. Thi, K. Koyama, K. Ohdaira, and H. Matsumura, *J. Appl. Phys.* **116**, 044510 (2014).
- 21) T. C. Thi, K. Koyama, K. Ohdaira, and H. Matsumura, *Jpn. J. Appl. Phys.* **55**, 02BF09

- (2016).
- 22) T. C. Thi, K. Koyama, K. Ohdaira, and H. Matsumura, Jpn. J. Appl. Phys. **53**, 022301 (2014).
 - 23) T. Oikawa, K. Ohdaira, K. Higashimine, and H. Matsumura, Curr. Appl. Phys. **15**, 1168 (2015).
 - 24) K. Ohdaira, T. C. Thi, and H. Matsumura, Jpn. J. Appl. Phys. **56**, 102301 (2017).
 - 25) S. Nishizaki, K. Ohdaira, and H. Matsumura Thin Solid Films **517**, 3581 (2009).
 - 26) T. Hayakawa, M. Miyamoto, K. Koyama, K. Ohdaira, H. Matsumura, Thin Solid Films **519**, 4466 (2011).
 - 27) R. Schorner and R. Hezel, IEEE Trans. Electron Devices **28**, 1466(1981)
 - 28) A. G. Aberle, Sol. Energy Mater. Sol. Cells **65**, 239(2001)
 - 29) P. V. Bulkin, P. L. Swart, and B. M. Lacquet, Thin Solid Films **241**, 247 (1994).
 - 30) G. Xu, P. Jin, M. Tazawa, and K. Yoshimura, Thin Solid Films **425**, 196 (2003).
 - 31) H. Umemoto, K. Ohara, D. Morita, T. Morimoto, M. Yamawaki, A. Masuda, and H. Matsumura, Jpn. J. Appl. Phys. **42**, 5315 (2003).
 - 32) J. -F. Lelièvre, E. Fourmond, A. Kaminski, O. Palais, D. Ballutaud, and M. Lemiti, Sol. Energy Mater. Sol. Cells **93**, 1281 (2009).
 - 33) F. Feldmann, M. Bivour, C. Reichel, H. Steinkemper, M. Hermle, S. W. Glunz, Sol. Energy Mater. Sol. Cells **131**, 46 (2014).

Table I. Deposition conditions of SiN_x films for the experiment to obtain thin SiN_x films.

Condition	Value
SiH ₄ flow rate (sccm)	3
NH ₃ flow rate (sccm)	50
H ₂ flow rate (sccm)	40
Gas pressure (Pa)	1
Substrate temperature (°C)	200
Catalyzer temperature (°C)	1800
Duration (s)	30–420

Table II. Deposition conditions of SiN_x films for the passivation of c-Si surfaces.

Condition	SiN _x	n-a-Si
SiH ₄ flow rate (sccm)	3	20
NH ₃ flow rate (sccm)	50	
H ₂ flow rate (sccm)	0–100	
PH ₃ (2.25% He-diluted) flow rate (sccm)		10
Gas pressure (Pa)	1	1
Substrate temperature (°C)	200	250
Catalyzer temperature (°C)	1800	1800
Duration (s)	30	60

Figure Captions

Fig. 1. (Color online) Thickness of SiN_x films as a function of deposition duration.

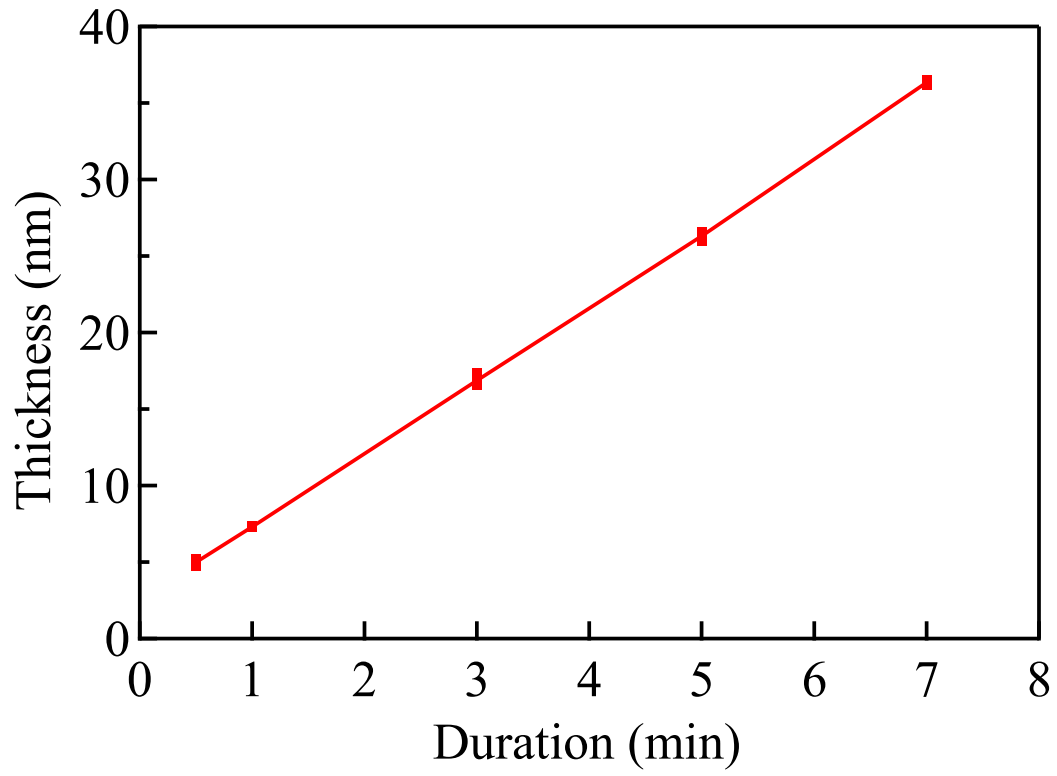
Fig. 2. (Color online) τ_{eff} of the samples with SiN_x layers as a function of the thickness of SiN_x layers.

Fig. 3. (Color online) τ_{eff} of the samples with SiN_x layers as a function of the duration of atomic hydrogen treatment.

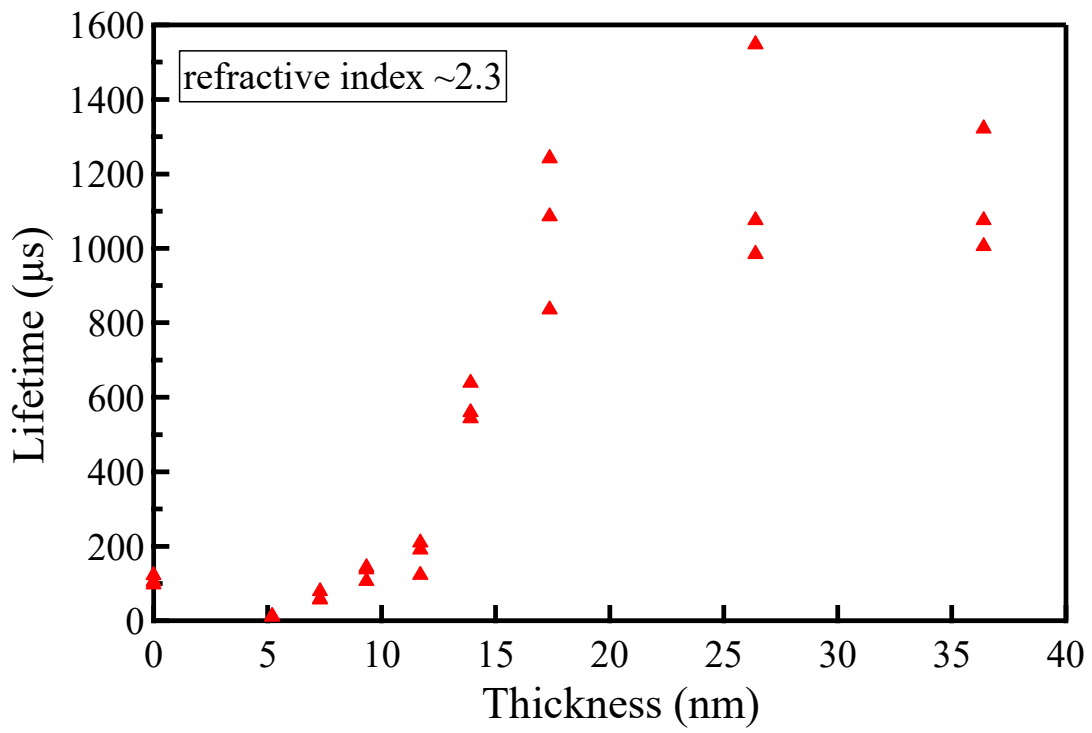
Fig. 4. (Color online) Thickness and refractive index of SiN_x layers as a function of H_2 flow rate during SiN_x deposition.

Fig. 5. (Color online) τ_{eff} of the samples passivated with SiN_x layers with different refractive index as a function of the duration of atomic hydrogen treatment.

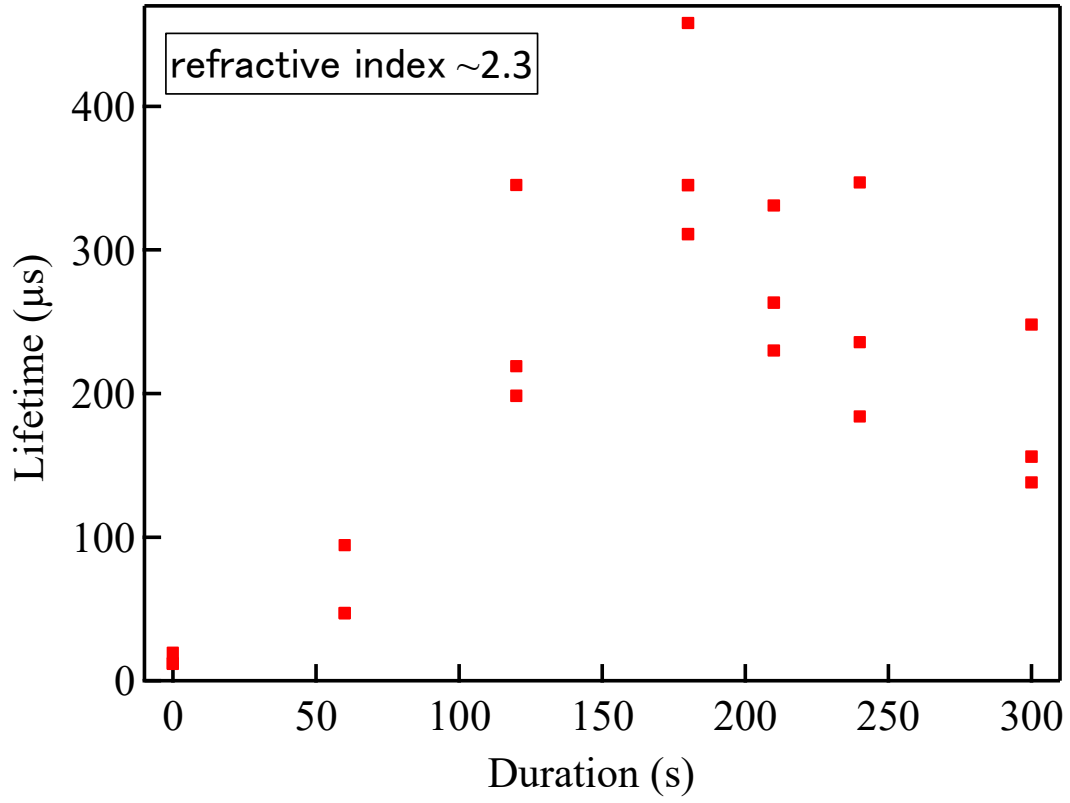
Fig. 6. (Color online) τ_{eff} of the samples passivated with SiN_x layers receiving atomic hydrogen treatment for 240 s as a function of the thickness of n-a-Si layers.



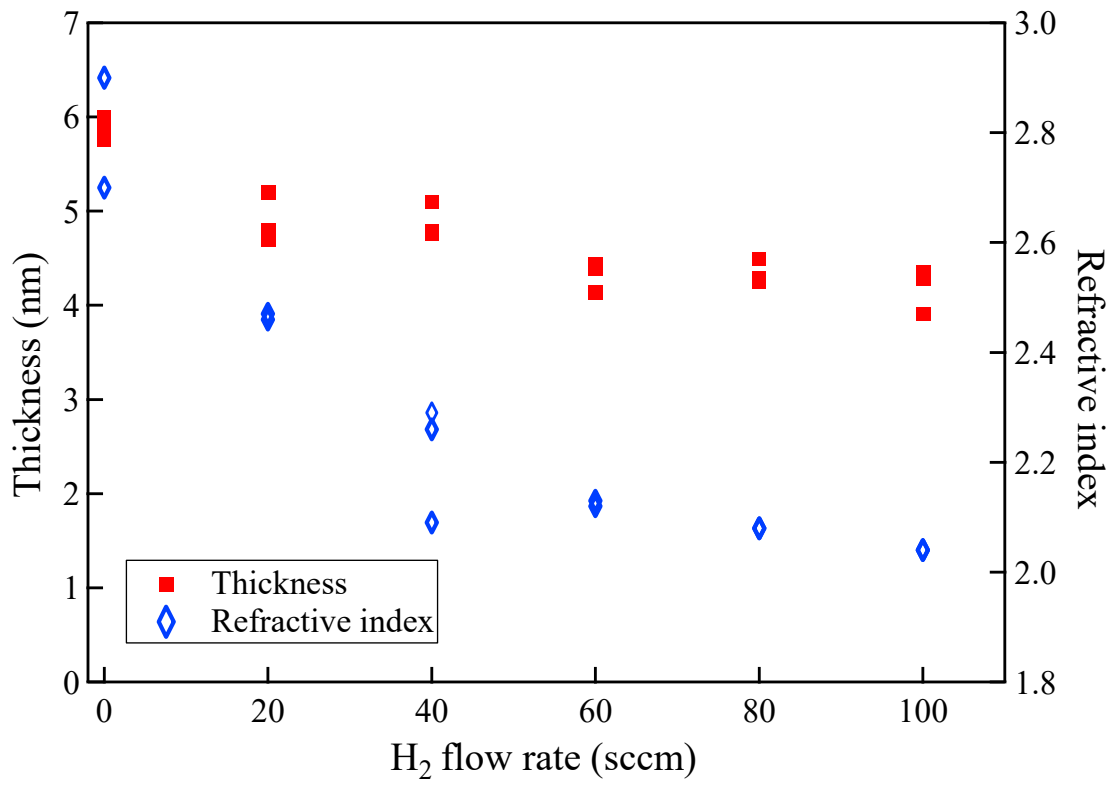
(Color online) Figure 1.



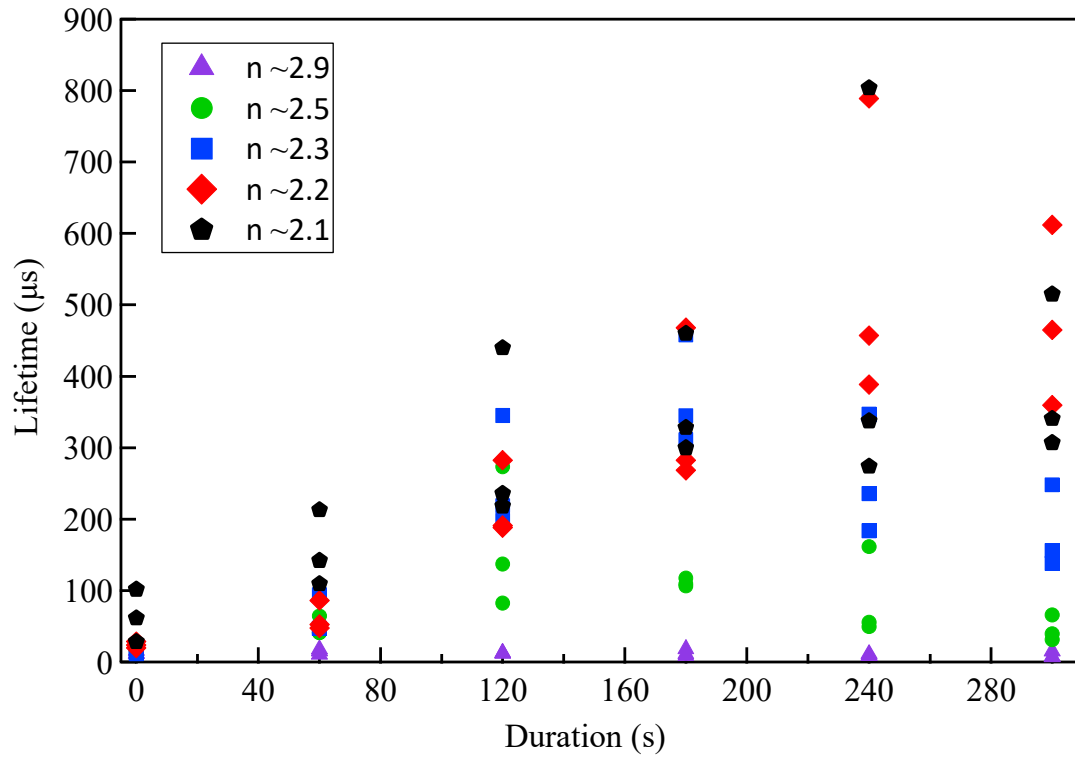
(Color online) Figure 2.



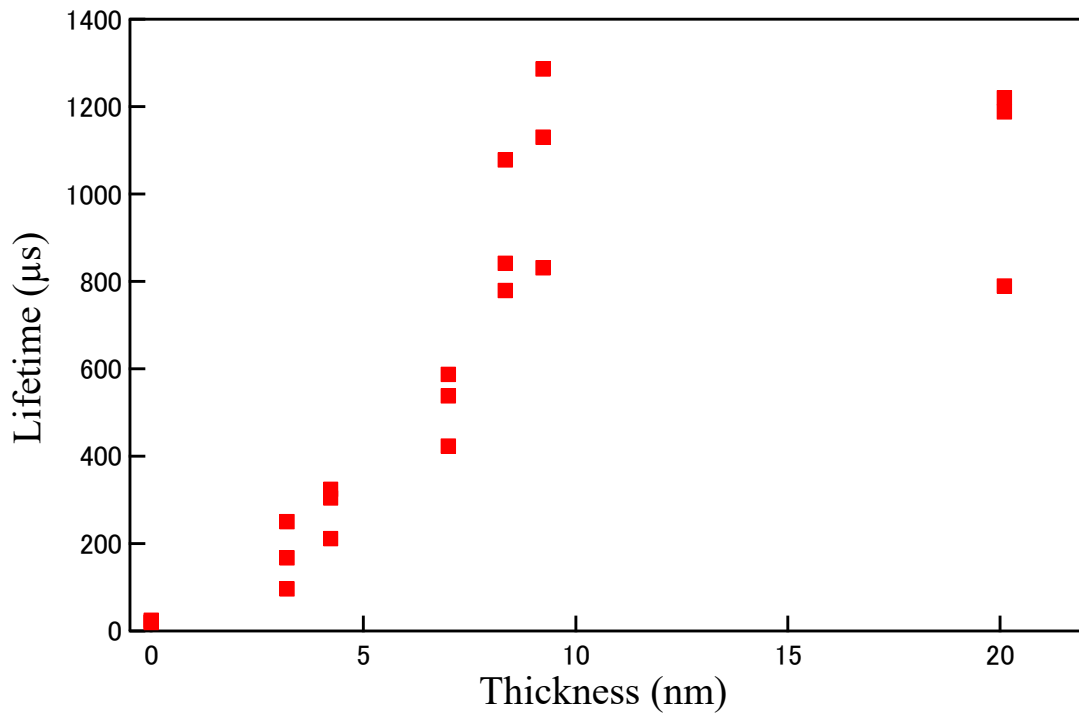
(Color online) Figure 3.



(Color online) Figure 4.



(Color online) Figure 5.



(Color online) Figure 6.